

Stably stratified magnetized stars in general relativity

Shijun Yoshida¹, Kenta Kiuchi², and Masaru Shibata²

¹*Astronomical Institute, Tohoku University, Sendai 980-8578, Japan*

²*Yukawa Institute for Theoretical Physics, Kyoto University, Kyoto 606-8502, Japan*

We construct magnetized stars composed of a fluid stably stratified by entropy gradients in the framework of general relativity, assuming ideal magnetohydrodynamics and employing a barotropic equation of state. We first revisit basic equations for describing stably-stratified stationary axisymmetric stars containing both poloidal and toroidal magnetic fields. As sample models, the magnetized stars considered by Ioka and Sasaki [23], inside which the magnetic fields are confined, are modified to the ones stably stratified. The magnetized stars newly constructed in this study are believed to be more stable than the existing relativistic models because they have both poloidal and toroidal magnetic fields with comparable strength, and magnetic buoyancy instabilities near the surface of the star, which can be stabilized by the stratification, are suppressed.

PACS numbers: 04.40.Dg, 97.60.Jd

I. INTRODUCTION

Recent observations established that soft-gamma repeaters (SGRs) and anomalous x-ray pulsars (AXPs) are the so-called magnetars, i.e., highly magnetized neutron stars whose surface field strength is as large as $\sim 10^{14} - 10^{15}$ G [1–5]. The presence of the magnetars has activated studies on equilibrium configurations of magnetized stars, which have a long history.

Since the pioneering work by Chandrasekhar and Fermi [6], an enormous number of studies has been done for exploring structures of magnetized stars: Prendergast [7] and Woltjer [8] calculated equilibrium configurations of magnetized stars having mixed poloidal-toroidal fields, where the magnetic fields are treated as first-order perturbations around a spherical star (see, also, Ref. [9]). Monaghan [10] studied magnetized stars containing purely poloidal magnetic fields. Ioka [11] developed the works by Prendergast and Woltjer into those of second-order perturbations to study magnetic effects on the stellar structures. He also employed the results obtained to explain magnetar activities. Miketinac obtained magnetized stars containing purely toroidal fields [12] and purely poloidal fields [13] by solving exact master equations numerically. Tomimura and Eriguchi developed a numerical method for obtaining magnetized stars with mixed poloidal-toroidal fields using a non-perturbative technique [14] (see, also, Refs. [15–17]). Duez and Mathis variationally considered the lowest-energy equilibrium states for a fixed magnetic helicity and constructed equilibria of magnetized stars having mixed poloidal-toroidal fields by a perturbation technique [18].

General relativistic models of magnetized neutron stars have been also explored. Bocquet et al. [19] and Cardall et al. [20] obtained relativistic neutron star models with purely poloidal magnetic fields. Using a perturbative technique, Konno et al. [21] calculated similar models. Kiuchi and Yoshida [22] computed magnetized stars with purely toroidal fields. Ioka and Sasaki [23], Colaiuda et al. [24], and Cioffi et al. [25, 26] derived relativistic stellar

models having both toroidal and poloidal magnetic fields with a perturbative technique. Although progress has been achieved in this field, further studies are required because all the magnetized star models are constructed by some special magnetic-field configurations which may not be realistic. In particular, it is not clear at all whether their models are stable.

The stability of the magnetized star is an important issue, because only stable equilibrium models are viable. Stability analyses of magnetized stars have been performed by many works, since the pioneering work by Tayler [27], who showed that stars having purely toroidal magnetic fields are unstable. Wright [28] subsequently showed that there is the same type of the instability, the so-called pinch-type instability, for stars containing purely poloidal magnetic fields. He also suggested the possibility that stars having mixed poloidal-toroidal magnetic fields may be stable if the strength of both components is comparable (see, also, Refs. [29, 30]). Assche et al. [31] proved that the pinch-type instability in general arises in magnetized stars with purely poloidal fields, and Wright [28] and Markey and Tayler [29] studied this instability for particular magnetic-field configurations. Flowers and Ruderman [32] found that another type of instability occurs in purely poloidal magnetic-field configurations.

All those classical stability analyses have been done by a method of an energy principle in the framework of Newtonian dynamics (see, also, Refs. [33, 34]). Another approach is a local analysis, with which Acheson [35] investigated the stability of rotating magnetized stars containing purely toroidal fields in detail in the framework of Newtonian dynamics (see, also, Refs. [36, 37]) and derived detailed stability conditions for purely toroidal magnetic fields buried inside rotating stars with dissipation. Note that although it is an approximate approach, the local analysis can take account of realistic effects on the stability like rotation, heat conduction, and resistivity, which cannot be included in a method of the energy principle. Bonanno and Urpin analyzed the axisymmetric stability [38] and the non-axisymmetric stabil-

ity [39] of cylindrical equilibrium configurations possessing mixed poloidal-toroidal fields, while ignoring compressibility and stratification of the fluid.

Recently the stability problem of the magnetized star has been approached from another direction. By following the time evolution of small random initial magnetic fields around a spherical star in the framework of Newtonian resistive magnetohydrodynamics, Braithwaite and Spruit [40, 41] obtained stable configurations of a magnetized star that are formed as a self-organization phenomenon. The resulting stable magnetic fields have both poloidal and toroidal components with comparable strength and support the conjecture for stability conditions of the magnetized star given by the classical studies mentioned before. By using the numerical magnetohydrodynamics simulation, Braithwaite [42] studied stability conditions for the magnetized stars and obtained a stability condition for his models given in terms of the ratio of the poloidal magnetic energy to the total magnetic energy which is of order unity. Duez et al. showed that magnetized stars constructed in Ref. [18] exhibit no instability for several Alfvén time scales in their numerical simulations [43]. This fact reconfirms the results given by Braithwaite. Lander and Jones explored the stability of magnetized stars by numerically solving the time evolution of linear perturbations around the stars in their series of papers [44–46]. For the purely toroidal/poloidal field cases, their results are consistent with those of the classical stability analysis, i.e., the pinch-type instability is observed near the symmetry and the magnetic axes for the purely toroidal and purely poloidal field cases, respectively. They also assessed the stability of various magnetized stars with mixed poloidal-toroidal fields and found that all their models considered suffer from the pinch-type instability even for the cases in which the poloidal and toroidal components have comparable strength [46]. It is obvious that the results by Lander and Jones are incompatible with those by Braithwaite and his collaborators [42, 43]. Lander and Jones discussed the possibility that some physics missing in their study would suppress the instability they found. We infer that in particular, *stratification of the fluid* will be a key ingredient, which is taken into account in the analyses of Refs. [42, 43] but not in the analyses of Ref. [46]. We will return to this point later.

General relativistic magnetized stars have been also analyzed recently. By numerical-relativity simulations, Kiuchi et al. [47, 48] investigated the stability of the magnetized stars with purely toroidal magnetic fields obtained by Kiuchi and Yoshida [22]. They showed that the stars with some specific distributions of magnetic fields are stable against axisymmetric perturbations but all the models considered are unstable against non-axisymmetric perturbations due to the strong magnetic buoyancy instability near the surface of the stars. The initial behavior of the instability observed in Refs. [47, 48] is consistent with that expected by the Newtonian linear analyses by Acheson [35]. Lasky et al. [49] and Cioffi et

al. [50] showed by numerical-relativity simulations that the purely poloidal magnetic fields, obtained by Bocquet et al. [19], are unstable due to the pinch-type instability near the magnetic axis as predicted by the Newtonian linear analyses [28, 29].

All these recent general relativistic magnetohydrodynamics simulations have contributed a lot to the progress of the stability analyses of general relativistic magnetized stars. However, the numerical simulations have been performed for equilibrium stars composed of *non-stratified* fluids. The assumption of non-stratification is often used and quite reasonable as a first approximation for exploring cold neutron stars, even though the cold neutron star is expected to be highly stably stratified by the composition gradient (see, e.g., Refs. [51–53]). If the effects of magnetic fields are taken into account for the neutron star models in their stability analysis, however, the situation changes drastically. As discussed by many authors, e.g., Reisenegger [54] and Kiuchi et al. [48], it has long been known that the magnetic buoyancy makes the magnetized star unstable and that the stable stratification is necessary to remove the magnetic buoyancy instability (the so-called Parker instability [55]). It should be emphasized that in the assumption that the stellar matter is stably stratified, Braithwaite and Spruit [40, 41] obtained stable magnetized stars of simple magnetic configurations in their numerical simulations. Therefore, we infer that a stable stratification is one of the key ingredients for stable configurations of the magnetized stars. Note that Lander and Jones [46] indicated the possibility that for stars containing mixed poloidal-toroidal magnetic fields, some weak instability associated with poloidal magnetic fields may not be removed by stable stratification (see, also, Ref. [38]). However, at the moment, no definite conclusion has been obtained. A reason that non-stratified magnetized stars are employed for the stability analyses in general relativity is that no model of stratified magnetized stars have been constructed, although in the framework of Newtonian dynamics, magnetized stars with stable stratification due to composition gradients have been obtained [56–58].

In this paper, thus, we study stably stratified and magnetized stars in the framework of general relativity aiming at giving a prescription for constructing them. First of all, we describe a general formulation to obtain stationary axisymmetric magnetized stars composed of both toroidal and poloidal magnetic fields with stratification due to entropy gradients assuming ideal magnetohydrodynamics and employing a barotropic equation of state. As sample models, the magnetized stars considered by Ioka and Sasaki [23], which contain poloidal and toroidal fields of comparable strength only inside the stars, are modified to be the ones stably stratified. Note that to date, no general relativistic magnetized stars containing mixed poloidal-toroidal fields have been constructed with a non-perturbative approach because of difficulties in the treatment of non-circular spacetimes (see, e.g., Ref. [59]). Finally, we describe the reason that the magnetized stars

obtained in the present study are more stable than the existing relativistic models.

II. BASIC EQUATIONS FOR THE GENERAL RELATIVISTIC IDEAL MAGNETOHYDRODYNAMICS

We consider perfect fluids coupled with electromagnetic fields, described by the basic equations summarized as follows. The baryon mass conservation equation:

$$\nabla_\mu(\rho u^\mu) = 0, \quad (1)$$

where ρ and u^μ are the rest-mass density and the fluid four velocity, respectively with ∇_μ being the covariant derivative associated with the metric $g_{\mu\nu}$. The two sets of the Maxwell equations:

$$\nabla_\alpha F_{\mu\nu} + \nabla_\mu F_{\nu\alpha} + \nabla_\nu F_{\alpha\mu} = 0, \quad (2)$$

$$\nabla_\nu F^{\mu\nu} = 4\pi J^\mu, \quad (3)$$

where $F_{\mu\nu}$ and J^μ are the Faraday tensor and the current four vector, respectively. The total energy-momentum conservation law:

$$\nabla_\nu T^{\mu\nu} = 0, \quad (4)$$

where $T^{\mu\nu}$ is the total energy-momentum tensor, defined by

$$T^{\mu\nu} = \rho h u^\mu u^\nu + P g^{\mu\nu} + \frac{1}{4\pi} \left[F^{\mu\alpha} F^\nu{}_\alpha - \frac{1}{4} g^{\mu\nu} F^{\alpha\beta} F_{\alpha\beta} \right], \quad (5)$$

with h and P being the specific enthalpy and the pressure, respectively. Here, the specific enthalpy is written, in terms of the specific internal energy ε , the pressure P , and the rest-mass density ρ , by

$$h \equiv 1 + \varepsilon + P/\rho. \quad (6)$$

It is convenient to introduce the electric field E_μ and the magnetic field B_μ observed by an observer associated with the matter four velocity u^μ , defined by

$$E_\mu = F_{\mu\nu} u^\nu, \quad (7)$$

$$B_\mu = -\frac{1}{2} \epsilon_{\mu\nu\alpha\beta} u^\nu F^{\alpha\beta}, \quad (8)$$

where $\epsilon_{\mu\nu\alpha\beta}$ is the Levi-Civita tensor with $\epsilon_{0123} = \sqrt{-g}$ with g being the determinant of the metric $g_{\mu\nu}$. In a large number of intriguing astrophysical problems, fluids coupled with electromagnetic fields can be approximated with perfectly conductive ones. Thus, we further assume the condition of perfect conductivity,

$$E_\mu = F_{\mu\nu} u^\nu = 0. \quad (9)$$

The dual tensor of $F^{\mu\nu}$ is then

$$F^{*\mu\nu} = \frac{1}{2} \epsilon^{\mu\nu\alpha\beta} F_{\alpha\beta} = B^\mu u^\nu - B^\nu u^\mu. \quad (10)$$

Equation (4) is often decomposed into two sets of equations, the energy equation and the momentum equation in the fluid rest frame, respectively, given by

$$\begin{aligned} -u_\mu \nabla_\nu T^{\mu\nu} &= u^\nu \nabla_\nu \{\rho(1 + \varepsilon)\} + \rho h \nabla_\nu u^\nu \\ &= \rho u^\nu \nabla_\nu \varepsilon + P \nabla_\nu u^\nu = 0, \end{aligned} \quad (11)$$

$$q_{\mu\alpha} \nabla_\nu T^{\alpha\nu} = \rho h u^\nu \nabla_\nu u_\mu + q_\mu^\nu \nabla_\nu P - F_{\mu\nu} J^\nu = 0 \quad (12)$$

where $q_{\mu\nu} \equiv g_{\mu\nu} + u_\mu u_\nu$. The perfect conductivity condition has been used to derive Equations (11) and (12). Using Equation (1) and the first law of thermodynamics,

$$d\varepsilon = \frac{P}{\rho^2} d\rho + T dS, \quad (13)$$

Equation (11) is recasted into the entropy equation,

$$u^\nu \nabla_\nu S = 0, \quad (14)$$

where S and T are the specific entropy and the temperature, respectively.

To construct a magnetized star, we employ barotropic equations of state given by

$$P = P(\rho), \quad \varepsilon = \varepsilon(\rho). \quad (15)$$

This equation of state is often used when studying a realistic star.

It should be noted that non-stratified isentropic fluids, characterized by $d\varepsilon = \rho^{-2} P d\rho$, have been assumed in a large number of studies of neutron stars in general relativity. When studying cold neutron stars in a chemical equilibrium, this simplification may be accepted. However, this is not the case if effects of magnetic fields are taken into account. As pointed out by many authors (see, e.g., Refs. [54] and [48]), the stable stratification is a necessary condition for magnetized stars to be stable. The reason is that magnetic flux tubes inside the star basically suffer from magnetic buoyancy and are forced to move toward their surface, resulting in a desperate instability of the stars. To counteract this magnetic buoyancy and to stabilize the stars, the stable stratification is required. For sufficiently cold neutron stars, the proton-neutron composition gradient is a candidate for the stratification [51]. When studying on the structure of a magnetized star, therefore, it is crucial to take into account this effect. Thus, the condition, $d\varepsilon = \rho^{-2} P d\rho$, which implies that the star is non-stratified, should not be a priori assumed. Note that whether the star is barotropic or not is independent of whether the star is stably stratified or not. With the one-parameter equation of state (15), it is possible to have a stably stratified star.

III. MASTER EQUATIONS FOR EQUILIBRIUM MAGNETIZED STARS WITH STABLE STRATIFICATIONS

In this section, we derive the master equations for describing stably stratified axisymmetric rotating stars

composed of mixed poloidal-toroidal magnetic fields. We take the time and azimuthal coordinates as $x^0 = t$ and $x^3 = \varphi$, respectively. Then, components of the two Killing vectors may be written as $t^\mu = \delta_0^\mu$ and $\varphi^\mu = \delta_3^\mu$, where δ_ν^μ is the Kronecker delta. The other two spatial coordinate variables are written as x^1 and x^2 in this section. Thus, the quantities describing the equilibrium stars are basically functions of x^1 and x^2 only. Henceforth, capital Latin indices (A, B, C, \dots) run from 1 to 2.

Because of the assumption of the axial symmetry and stationarity, Equation (14) is written as

$$u^A \partial_A S = 0. \quad (16)$$

This equation means that the specific entropy has to be constant along streamlines on the stellar meridional plane unless $u^A = 0$. However, the constant specific entropy distribution along streamlines is not realized for stable magnetized stars because of the following reason: For stationary axisymmetric stars, streamlines on the meridional plane, in general, are closed curves. Thus, it is inevitable that there exists an unstably stratified region (convectively unstable region) where $(\nabla^\mu P)(\nabla_\mu S) < 0$ is satisfied. To construct a stably stratified (convectively stable) star, thus, we have to assume

$$u^A = 0. \quad (17)$$

Then, we have no condition for S apart from the assumption of the stationarity and the axial symmetry. In other words, we can freely choose a functional form of S if $u^A = 0$ is assumed.

The assumption, $u^A = 0$, is an essential difference between our study and the study of Ref. [23] in which the *isentropic* meridional flow is taken into account. The fluid four-velocity is, thus, given by

$$u^\mu = \gamma(t^\mu + \Omega \varphi^\mu). \quad (18)$$

where Ω is the angular velocity of the fluid and $\gamma = u^0$.

From Equations (2), (9), and the integrability condition for the momentum equation (12), we have the following relations:

$$F_{A3} = \frac{\partial}{\partial x^A} \Psi, \quad (19)$$

$$F_{03} = 0, \quad (20)$$

$$F_{0A} = -\Omega_F(\Psi) F_{3A}, \quad (21)$$

$$\sqrt{-g} F^{12} = \hat{\Gamma}(\Psi), \quad (22)$$

$$-\Omega_F(\Psi) u^0 + u^3 = 0, \quad (23)$$

$$-\ln \gamma + \int \frac{dP}{\rho h} - \int \mu(\Psi) d\Psi + \hat{C} = 0, \quad (24)$$

$$J^3 - \Omega_F J^0 = \rho h \{ \mu(\Psi) + \gamma u_3 \Omega'_F \} + \frac{F_{12}}{4\pi\sqrt{-g}} \hat{\Gamma}', \quad (25)$$

where Ω_F , $\hat{\Gamma}$, and μ are arbitrary functions of the flux function Ψ , which is the azimuthal component of the vector potential A_μ associated with $F_{\mu\nu}$ as shown in Equation (19). Here, \hat{C} is an integral constant, and the prime denotes the derivative with respect to Ψ . Note that Ω_F is sometimes called the angular velocity of the magnetic field line. Substituting Equation (18) into Equation (23), we obtain

$$\Omega_F = \Omega. \quad (26)$$

Equation (24) corresponds to the equation of the hydrostatic equilibrium.

For cases of non-stratified stars, the present formulation may be derived from that of Ioka and Sasaki [23] by taking a limit. First, we focus on Equations (16) – (18) of Ref. [23]. Using a relation

$$\gamma(u_0 + \Omega u_3) = -1, \quad (27)$$

or $u^\mu u_\mu = -1$, we may rewrite Equation (24) as

$$(u_0 + \Omega u_3) e^{\int \frac{dP}{\rho h}} = -e^{\int \mu(\Psi) d\Psi - \hat{C}}, \quad (28)$$

which corresponds to Equation (16) of Ref. [23]. We therefore found that functions μ and D in Ref. [23] correspond to $\exp(\int \frac{dP}{\rho h})$ and $\exp(\int \mu(\Psi) d\Psi - \hat{C})$, respectively. Note that μ of Ref. [23] is exactly the same as h of the present study and that $h^{-1} dh = (\rho h)^{-1} dP$ in the isentropic case $d\varepsilon = \rho^{-2} P d\rho$. Equations (17) and (18) of Ref. [23] are, respectively, derived from the energy and angular momentum conservation equations,

$$\nabla_\mu (T^\mu{}_\nu t^\nu) = 0, \quad \nabla_\mu (T^\mu{}_\nu \varphi^\nu) = 0. \quad (29)$$

These may be explicitly written by

$$\nabla_\mu (\rho h u_\nu \xi^\nu u^\mu) + \nabla_\mu \left[\frac{1}{4\pi} F^{\mu\alpha} F_{\nu\alpha} \xi^\nu \right] = 0, \quad (30)$$

with ξ^μ being t^μ or φ^μ . Since we assume the condition (17), the first term in the left-hand side of Equation (30) automatically vanishes and we obtain two relations,

$$X = \sqrt{-g} F^{12} \Omega, \quad Y = \sqrt{-g} F^{12}, \quad (31)$$

where X and Y are arbitrary functions of the flux function Ψ . These relations were already derived in Equations (21) and (22). Thus, we find that $X = \hat{\Gamma} \Omega$ and $Y = \hat{\Gamma}$. The functions X and Y are, in terms of the functions of Ref. [23], C , E , and L , given by

$$X = -4\pi \frac{E}{C}, \quad Y = -4\pi \frac{L}{C}. \quad (32)$$

From Equation (20) of Ref. [23], we have $D/C = E/C - \Omega L/C$. As argued in Ref. [23], the no-meridional flow

limit of magnetized stars with mixed poloidal-toroidal magnetic fields is given by the limit $C \rightarrow \infty$ with $D, L/C$ and E/C kept to be finite. Thus, we find that $D/C = E/C - \Omega L/C$ becomes $0 = -4\pi E/C + 4\pi \Omega L/C = X - \Omega Y$ in this limit, which is automatically satisfied by Equation (31) in the present situation.

Once the metric coefficients are given, all the components of $F^{\mu\nu}$ are written as functions of Ψ and $\partial\Psi/\partial x^A$ through the two arbitrary functions of the flux function, Ω_F and $\hat{\Gamma}$. Using the Maxwell equation (3), thus, $J^0 - \Omega_F J^3$ appearing in the left-hand side of Equation (25) can be written as a second-order elliptic-type partial differential operator for $\Psi(x^1, x^2)$. Equation (3) in conjunction with Equation (25) may then be solved to obtain a distribution of the magnetic fields around a star. This equation is often called the Grad-Shafranov (GS) equation [60] when it is written as a partial differential equation for Ψ .

It is useful to introduce some global quantities to characterize equilibrium solutions of stars. For equilibrium states of magnetized stars, the total baryon rest mass \widetilde{M}^* , the internal thermal energy $\widetilde{E}_{\text{int}}$, and the electro-magnetic energy $\widetilde{E}_{\text{EM}}$ may be defined as

$$\widetilde{M}^* = \int \rho \gamma \sqrt{-g} d^3x, \quad (33)$$

$$\widetilde{E}_{\text{int}} = \int \rho \varepsilon \gamma \sqrt{-g} d^3x, \quad (34)$$

$$\widetilde{E}_{\text{EM}} = \frac{1}{8\pi} \int B^\mu B_\mu \gamma \sqrt{-g} d^3x. \quad (35)$$

(see, e.g., Ref. [22].)

IV. MAGNETIC FIELDS AROUND A SPHERICAL STAR AND THEIR EFFECTS ON THE STELLAR STRUCTURES

A. Spherical stars with no magnetic field

We assume that the magnetic energy density is much smaller than the matter density and pressure so that the magnetic-field effects can be treated as perturbations on a spherical non-magnetized star. The background metric is then given by

$$ds^2 = -e^{2\nu} dt^2 + e^{2\lambda} dr^2 + r^2(d\theta^2 + \sin^2\theta d\varphi^2), \quad (36)$$

where ν and λ are functions of r [61]. The function γ for the spherical stars is written as

$$\gamma = e^{-\nu}. \quad (37)$$

The equilibrium state of a star is described by the set of the following TOV equations [61]:

$$\frac{dm}{dr} = 4\pi r^2 \rho(1 + \varepsilon), \quad (38)$$

$$\frac{dP}{dr} = -e^{2\lambda} \rho h \frac{m + 4\pi P r^3}{r^2}, \quad (39)$$

$$\frac{d\nu}{dr} = -\frac{1}{\rho h} \frac{dP}{dr}, \quad (40)$$

where m is defined by

$$m \equiv \frac{r}{2}(1 - e^{-2\lambda}). \quad (41)$$

For the unperturbed spherical stars, the gravitational mass M , the total baryon rest mass M^* , and the internal thermal energy E_{int} are given by

$$M = m(R), \quad (42)$$

$$M^* = 4\pi \int_0^R \rho e^\lambda r^2 dr, \quad (43)$$

$$E_{\text{int}} = 4\pi \int_0^R \rho \varepsilon e^\lambda r^2 dr, \quad (44)$$

where R denotes the circumferential radius of the star defined by $P(R) = 0$. The gravitational potential energy W for the unperturbed stars is defined by

$$|W| = M^* + E_{\text{int}} - M. \quad (45)$$

B. Magnetic field around a spherical star

A profile of magnetic fields is determined by specifying the functional forms of Ω_F , $\hat{\Gamma}$, and μ , which are the arbitrary functions of Ψ . Following Ioka and Sasaki [23], we assume that these three functions as well as the integral constant, \hat{C} , are given by

$$\Omega_F = \Omega = \Omega_2 \Psi^2, \quad (46)$$

$$\mu = C_1, \quad (47)$$

$$\hat{\Gamma} = L\Psi, \quad (48)$$

$$\hat{C} = C_0 + C_2, \quad (49)$$

where Ω_2 , C_0 , C_1 , C_2 , and L are constants. Because we consider weak magnetic fields around a spherical star, it is useful to introduce a smallness parameter η for which $\Psi = O(\eta)$. For the constants appearing in Equations (46) – (49), we further assume that

$$\begin{aligned} \Omega_2 &= O(1), \quad C_0 = O(1), \quad C_1 = O(\eta), \\ C_2 &= O(\eta^2), \quad L = O(1), \end{aligned} \quad (50)$$

C_0 is determined in the background equation for Equation (24). Then, up to the first order in η , $F_{\mu\nu}$ is written as

$$F_{\mu\nu} = \begin{pmatrix} 0 & 0 & 0 & 0 \\ 0 & 0 & e^{\lambda-\nu} L \csc\theta \Psi & \partial_r \Psi \\ 0 & -e^{\lambda-\nu} L \csc\theta \Psi & 0 & \partial_\theta \Psi \\ 0 & -\partial_r \Psi & -\partial_\theta \Psi & 0 \end{pmatrix}, \quad (51)$$

and Equation (25) becomes

$$J^3 = \rho h C_1 + \frac{e^{-2\nu} L^2 \Psi}{4\pi r^2 \sin^2\theta}. \quad (52)$$

Note that the contribution of Ω_2 is neglected because it is a higher-order quantity. In terms of Ψ , J^3 is given by

$$\begin{aligned} J^3 &= \frac{1}{4\pi} \nabla_\alpha F^{3\alpha} \\ &= -\frac{1}{4\pi e^{\nu+\lambda} r^2 \sin^2 \theta} \left[\frac{\partial}{\partial r} \left(e^{\nu-\lambda} \frac{\partial}{\partial r} \Psi \right) \right. \\ &\quad \left. + \frac{e^{\nu+\lambda}}{r^2} \sin \theta \frac{\partial}{\partial \theta} \left(\frac{1}{\sin \theta} \frac{\partial}{\partial \theta} \Psi \right) \right]. \end{aligned} \quad (53)$$

From Equations (52) and (53), we obtain the master equation for the flux function Ψ (the GS equation),

$$\begin{aligned} e^{\lambda-\nu} \left[\frac{\partial}{\partial r} \left(e^{\nu-\lambda} \frac{\partial}{\partial r} \Psi \right) + \frac{e^{\nu+\lambda}}{r^2} \sin \theta \frac{\partial}{\partial \theta} \left(\frac{1}{\sin \theta} \frac{\partial}{\partial \theta} \Psi \right) \right] \\ + 4\pi r^2 \sin^2 \theta \rho h e^{2\lambda} C_1 + e^{2(\lambda-\nu)} L^2 \Psi = 0. \end{aligned} \quad (54)$$

Because it is the azimuthal component of the vector potential, the flux function Ψ may be expanded by the vector harmonics with the axial parity as

$$\Psi = 4\pi C_1 \sum_{l=1}^{\infty} r^{l+1} \psi_l(r) \sin \theta \frac{\partial}{\partial \theta} P_l(\theta), \quad (55)$$

where P_l is the Legendre polynomial (see, e.g., Ref. [62]). Substituting Equation (55) into the GS equation (54) yields

$$\begin{aligned} \frac{d^2 \psi_l}{dr^2} + \left(\frac{d(\nu-\lambda)}{dr} + \frac{2(l+1)}{r} \right) \frac{d\psi_l}{dr} \\ + \left[e^{2(\lambda-\nu)} L^2 + \frac{l(l+1)}{r^2} (1 - e^{2\lambda}) + \frac{d(\nu-\lambda)}{dr} \frac{l+1}{r} \right] \psi_l \\ - \rho h e^{2\lambda} \delta_l^1 = 0. \end{aligned} \quad (56)$$

Regular solutions of Equation (56) near the center of the star can be written as

$$\psi_l = a_0 + a_2 r^2 + \dots, \quad (57)$$

where a_0 and a_2 are constants with a_2 given by

$$\begin{aligned} a_2 = & -\frac{e^{-2\nu_0} L^2 - 2(l+1)[(l+1)\lambda_2 - \nu_2]}{2(2l+3)} a_0 \\ & + \frac{1}{10} \rho_0 h_0 \delta_l^1. \end{aligned} \quad (58)$$

Here, constants ν_0 , ν_2 , λ_2 , ρ_0 and h_0 are defined in the power series expansion of the background quantities near $r = 0$ as follows:

$$\nu = \nu_0 + \nu_2 r^2 + \dots, \quad (59)$$

$$\lambda = \lambda_2 r^2 + \dots, \quad (60)$$

$$h = h_0 + h_2 r^2 + \dots, \quad (61)$$

$$\rho = \rho_0 + \rho_2 r^2 + \dots. \quad (62)$$

Following Ref. [23], we focus on magnetized stars whose exterior is vacuum and whose surface has no magnetic field. At the surface of the star, then, we need to

require two boundary conditions for the flux function, given by

$$\psi_l = 0, \quad \frac{d\psi_l}{dr} = 0, \quad \text{at } r = R, \quad (63)$$

where R is the radius of the unperturbed star. For the $l \neq 1$ cases, Equation (56) becomes a homogeneous equation. In general, then, the three boundary conditions, the regularity condition at the center of the star and the surface boundary conditions given by Equation (63), cannot be satisfied simultaneously. In other words, we have to require $\psi_l = 0$ for $l \neq 1$. For the $l = 1$ case, due to the two boundary conditions at the stellar surface, given in Equation (63), the GS equation becomes an eigenvalue equation with respect to the two parameters a_0 and L . The other parameter C_1 can be assigned freely and determines the strength of the magnetic fields. The remaining constant C_2 is related to the pressure perturbation as discussed below.

The r and θ components of the vector potential A_μ may be obtained straightforwardly. If we set $A_\theta = 0$ by using a gauge degree of freedom, F_{12} is given by

$$\begin{aligned} F_{12} &= -\partial_\theta A_r \\ &= e^{\lambda-\nu} L \csc \theta \Psi \\ &= 4\pi C_1 e^{\lambda-\nu} L r^2 \psi_1(r) \frac{\partial}{\partial \theta} P_1(\theta). \end{aligned} \quad (64)$$

Requiring the regularity on the symmetry axis, we have

$$A_r = -4\pi C_1 e^{\lambda-\nu} L r^2 \psi_1(r) P_1(\theta). \quad (65)$$

If another gauge condition is required, we may make a gauge transformation

$$A_\mu \rightarrow A_\mu - \partial_\mu \{f(r) P_1(\theta)\}, \quad (66)$$

to obtain the vector potential that satisfies a required gauge condition.

C. Stellar deformation due to the magnetic fields

As discussed before, the flux function in the present situation is given by

$$\begin{aligned} \Psi &= 4\pi C_1 r^2 \psi_1(r) \sin \theta \frac{\partial}{\partial \theta} P_1(\theta) \\ &\equiv 4\pi C_1 \Psi_1(r) \left(\frac{2}{3} P_2(\theta) - \frac{2}{3} \right). \end{aligned} \quad (67)$$

Thus, the energy-momentum tensor associated with the electromagnetic fields $T_{(\text{em})\nu}^\mu$, defined by

$$T_{(\text{em})\nu}^\mu = \frac{1}{4\pi} \left[F^{\mu\alpha} F_{\nu\alpha} - \frac{1}{4} \delta_\nu^\mu F^{\alpha\beta} F_{\alpha\beta} \right], \quad (68)$$

induces a deviation of the order of $O(\eta^2)$ from the background spherical matter distribution. The line element

is then perturbed as follows:

$$\begin{aligned}
ds^2 = & -e^{2\nu} \left\{ 1 + 2 \sum_{i=0,2} (4\pi C_1)^2 H_i(r) P_i(\theta) \right\} dt^2 \\
& + e^{2\lambda} \left\{ 1 + 2 \frac{e^{2\lambda}}{r} \sum_{i=0,2} (4\pi C_1)^2 M_i(r) P_i(\theta) \right\} dr^2 \\
& + r^2 \{ 1 + 2(4\pi C_1)^2 K_2(r) P_2(\theta) \} (d\theta^2 + \sin^2 \theta d\varphi^2) \\
& + 2(4\pi C_1)^2 W_2(r) \sin \theta \partial_\theta P_2(\theta) dr d\varphi, \quad (69)
\end{aligned}$$

where H_i , M_i , K_i , I_i , V_i , $W_i = O(1)$ because $C_1 = O(\eta)$. Here, we employ the Regge-Wheeler gauge. In this perturbed spacetime, the function γ in Equation (18) is given by

$$\gamma = e^{-\nu} \left\{ 1 - \sum_{i=0,2} (4\pi C_1)^2 H_i(r) P_i(\theta) \right\} \quad (70)$$

because $\delta u^A = 0$ and δu^3 is the second-order quantity (see Equations (17) and (46)). Here, we have omitted the terms higher than $O(\eta^2)$. From Equation (24), the pressure perturbation δP is, in terms of the metric and the flux functions, written as

$$\begin{aligned}
\delta P & \equiv (4\pi C_1)^2 \sum_{i=0,2} \delta P_i(r) P_i(\theta) \\
& = \rho h \left\{ C_1 \Psi - C_2 - \sum_{i=0,2} (4\pi C_1)^2 H_i(r) P_i(\theta) \right\}. \quad (71)
\end{aligned}$$

Thus, we have

$$\delta P_0 = \rho h \left[-\frac{1}{6\pi} \Psi_1(r) - H_0(r) - \tilde{C}_2 \right], \quad (72)$$

$$\delta P_2 = \rho h \left[\frac{1}{6\pi} \Psi_1(r) - H_2(r) \right]. \quad (73)$$

where $\tilde{C}_2 \equiv C_2/(4\pi C_1)^2$.

We then obtain a set of the metric perturbation equations as follows:

$$\begin{aligned}
\frac{dM_0}{dr} & = 4\pi r^2 \rho h \left(\frac{d(\rho + \rho\varepsilon)}{dP} \right) \left(\frac{\delta P_0}{\rho h} \right) + \frac{1}{3} e^{-2\lambda} \left(\frac{d\Psi_1}{dr} \right)^2 \\
& + \frac{1}{3r^2} (2 + L^2 r^2 e^{-2\nu}) (\Psi_1)^2, \quad (74)
\end{aligned}$$

$$\begin{aligned}
\frac{dH_0}{dr} & = 4\pi r e^{2\lambda} \rho h \left(\frac{\delta P_0}{\rho h} \right) \\
& + \frac{e^{2\lambda}}{r^2} \left(1 + 2r \frac{d\nu}{dr} \right) M_0 + \frac{1}{3r} \left(\frac{d\Psi_1}{dr} \right)^2 \\
& + \frac{e^{2\lambda}}{3r^3} (-2 + L^2 r^2 e^{-2\nu}) (\Psi_1)^2, \quad (75)
\end{aligned}$$

$$W_2 = \frac{2}{3} L e^{\lambda-\nu} (\Psi_1)^2, \quad (76)$$

$$H_2 + \frac{e^{2\lambda} M_2}{r} = \frac{2e^{-2\lambda}}{3} \left(\frac{d\Psi_1}{dr} \right)^2 - \frac{2e^{-2\nu}}{3} L^2 (\Psi_1)^2, \quad (77)$$

$$\begin{aligned}
& \frac{1}{r} \left(\frac{dH_2}{dr} + \frac{dK_2}{dr} \right) + \frac{d\nu}{dr} \frac{dK_2}{dr} - 2 \frac{e^{2\lambda}}{r^2} (K_2 + H_2) \\
& - \frac{e^{2\lambda}}{r^2} H_2 - \frac{e^{2\lambda}}{r^3} \left(1 + 2r \frac{d\nu}{dr} \right) M_2 \\
& = 4\pi e^{2\lambda} \delta P_2 - \frac{1}{3r^2} \left(\frac{d\Psi_1}{dr} \right)^2 \\
& - \frac{e^{2\lambda}}{3r^4} (4 + L^2 r^2 e^{-2\nu}) (\Psi_1)^2, \quad (78)
\end{aligned}$$

$$\begin{aligned}
& \frac{dH_2}{dr} + \frac{dK_2}{dr} + \frac{1}{r} \left(-1 + r \frac{d\nu}{dr} \right) H_2 \\
& - \frac{e^{2\lambda}}{r^2} \left(1 + r \frac{d\nu}{dr} \right) M_2 = \frac{4}{3r^2} \Psi_1 \frac{d\Psi_1}{dr}. \quad (79)
\end{aligned}$$

For the perturbation with $l = 0$, it is convenient to obtain M_0 and $\delta P_0/(\rho h)$ first. The equation for determining $\delta P_0/(\rho h)$ is derived from Equations (72) and (75) as

$$\begin{aligned}
\frac{d}{dr} \left(\frac{\delta P_0}{\rho h} \right) & = -\frac{1}{6\pi} \frac{d\Psi_1}{dr} - \frac{dH_0}{dr} \\
& = -\frac{1}{6\pi} \frac{d\Psi_1}{dr} - 4\pi r e^{2\lambda} \rho h \left(\frac{\delta P_0}{\rho h} \right) \\
& - \frac{e^{2\lambda}}{r^2} \left(1 + 2r \frac{d\nu}{dr} \right) M_0 - \frac{1}{3r} \left(\frac{d\Psi_1}{dr} \right)^2 \\
& - \frac{e^{2\lambda}}{3r^3} (-2 + L^2 r^2 e^{-2\nu}) (\Psi_1)^2. \quad (80)
\end{aligned}$$

Following Ref. [23], a new dependent variable Y_2 is, for the perturbation with $l = 2$, introduced by

$$\begin{aligned}
Y_2 & \equiv H_2 + K_2 \\
& - \frac{e^{-2\lambda}}{6} \left\{ \left(\frac{d\Psi_1}{dr} \right)^2 + \frac{4}{r} \Psi_1 \frac{d\Psi_1}{dr} + \frac{4e^{2\lambda}}{r^2} (\Psi_1)^2 \right\}, \quad (81)
\end{aligned}$$

which facilitates the numerical computation. Then, two independent variables Y_2 and H_2 may be determined by

$$\begin{aligned}
\frac{dY_2}{dr} & = -2 \frac{d\nu}{dr} H_2 - \frac{r \rho h}{3} \left(2\Psi_1 + r \frac{d\Psi_1}{dr} \right) \\
& - \frac{2}{3} e^{-2\nu} L^2 \frac{d\nu}{dr} (\Psi_1)^2 + e^{-2\lambda} \frac{d\nu}{dr} \left(\frac{d\Psi_1}{dr} \right)^2 \\
& + \frac{1}{3r^2} \left[-2 + 2e^{-2\lambda} \left\{ 1 + r \frac{d(\nu + \lambda)}{dr} \right\} \right. \\
& \left. + e^{-2\nu} L^2 r^2 \right] \Psi_1 \frac{d\Psi_1}{dr}, \quad (82)
\end{aligned}$$

$$\begin{aligned}
\frac{d\nu}{dr} \frac{dH_2}{dr} &= \left\{ \frac{1}{r^2} (1 - e^{2\lambda}) - 2 \left(\frac{d\nu}{dr} \right)^2 + 4\pi e^{2\lambda} h \rho \right\} H_2 \\
&- 2 \frac{e^{2\lambda}}{r^2} Y_2 - \frac{2}{3} e^{2\lambda} \rho h \Psi_1 \\
&+ \frac{2}{3} e^{-2\lambda} \left(\frac{d\nu}{dr} \right)^2 \left(\frac{d\Psi_1}{dr} \right)^2 + \frac{4}{3r^2} \frac{d\nu}{dr} \Psi_1 \frac{d\Psi_1}{dr} \\
&+ \frac{e^{-2\nu} L^2}{3r^2} \left\{ e^{2\lambda} - 2r^2 \left(\frac{d\nu}{dr} \right)^2 \right\} (\Psi_1)^2.
\end{aligned} \tag{83}$$

Once Ψ_1 , $\delta P_0/(\rho h)$, M_0 , Y_2 , and H_2 are obtained, the other perturbation quantities may be calculated algebraically through Equations (72), (73), (76), (77), and (81).

Near the center of the star, the physically acceptable solutions may be expanded in the power series of r as

$$\delta P_0/(\rho h) = h_{00} + h_{02}r^2 + \dots, \tag{84}$$

$$M_0 = r^3(m_{00} + m_{02}r^2 + \dots), \tag{85}$$

$$Y_2 = r^4(y_{20} + y_{22}r^2 + \dots), \tag{86}$$

$$H_2 = r^2(h_{20} + h_{22}r^2 + \dots). \tag{87}$$

Here, we have two options for determining a value of h_{00} . One is to set $h_{00} = 0$, which corresponds to considering sequences of the magnetized stars characterized by the fixed central density. The other is to use h_{00} to keep the total baryon mass \tilde{M}^* constant for the magnetized stars. This corresponds to considering sequences of the magnetized stars characterized by the fixed total baryon mass. Following Ref. [23], we choose the latter option, i.e., on the constant baryon mass sequences of the magnetized stars.

Outside the star, the master equations become

$$\frac{dM_0}{dr} = 0, \tag{88}$$

$$\frac{dH_0}{dr} = \frac{M_0}{(r - 2M)^2}, \tag{89}$$

$$W_2 = 0, \tag{90}$$

$$H_2 + \frac{M_2}{r - 2M} = 0, \tag{91}$$

$$\frac{dY_2}{dr} = -\frac{2M}{r(r - 2M)} H_2, \tag{92}$$

$$\frac{dH_2}{dr} = -2 \left\{ \frac{1}{r} + \frac{M}{r(r - 2M)} \right\} H_2 - \frac{2}{M} Y_2. \tag{93}$$

For the $l = 0$ perturbation, the vacuum solutions are given by

$$M_0 = M_0(R) = \text{const.}, \quad H_0 = -\frac{M_0(R)}{r - 2M}. \tag{94}$$

As for the $l = 2$ perturbation, manipulating Equations (92) and (93) yields

$$\begin{aligned}
&-(y + 1)(y - 1) \frac{d^2 H_2}{dy^2} - 2y \frac{dH_2}{dy} \\
&+ \left\{ 6 + \frac{4}{(y + 1)(y - 1)} \right\} H_2 = 0,
\end{aligned} \tag{95}$$

where $y \equiv r/M - 1$. This is the associated Legendre equation. Since $\lim_{y \rightarrow \infty} H_2 = 0$ for physically acceptable solutions, we obtain

$$H_2 = DQ_2^2(y), \tag{96}$$

where Q_l^m and D are the associated Legendre function of the second kind and a constant, respectively. With a recurrence relation for Q_l^m ,

$$\frac{dQ_l^m}{dy} = \frac{(l + m)(l - m + 1)}{\sqrt{y^2 - 1}} Q_l^{m-1} - \frac{my}{y^2 - 1} Q_l^m. \tag{97}$$

we have

$$Y_2 = -\frac{2D}{\sqrt{y^2 - 1}} Q_2^1(y). \tag{98}$$

At the surface of the star, the outer solutions, given by (94), (96) and (98), are matched to the inner solutions integrated from the center of the star with the boundary conditions (84) – (87).

D. Global quantities characterizing magnetized stars

As mentioned before, the global physical quantities (33) – (35) are useful for exploration of the magnetized star. Perturbations due to the magnetic effects in the gravitational mass, the total baryon rest mass \tilde{M}^* , and the internal thermal energy \tilde{E}_{int} are, respectively, given by

$$\Delta M = (4\pi C_1)^2 M_0(R), \tag{99}$$

$$\begin{aligned}
\Delta M^* &= 4\pi (4\pi C_1)^2 \\
&\times \int_0^R \rho e^\lambda r^2 \left(\frac{d \ln \rho}{dP} \delta P_0 + \frac{e^{2\lambda} M_0}{r} \right) dr,
\end{aligned} \tag{100}$$

$$\begin{aligned}
\Delta E_{\text{int}} &= 4\pi (4\pi C_1)^2 \\
&\times \int_0^R \rho \varepsilon e^\lambda r^2 \left(\frac{d \ln(\rho \varepsilon)}{dP} \delta P_0 + \frac{e^{2\lambda} M_0}{r} \right) dr
\end{aligned} \tag{101}$$

As already mentioned, we study the sequences of equilibrium states of the magnetized star characterized by the fixed total baryon mass. Thus, the condition of $\Delta M^* = 0$ is employed for determining values of h_{00} in Equation (84), which is related to the perturbations in the central density of the star, $\Delta \rho_c$, through the relation

$$\Delta \rho_c = (4\pi C_1)^2 \rho h \frac{d\rho}{dP} \Big|_{r=0} h_{00}. \tag{102}$$

The electromagnetic energy E_{EM} is decomposed as

$$E_{\text{EM}} = E_{\text{EM}}^{(p)} + E_{\text{EM}}^{(t)}, \quad (103)$$

where $E_{\text{EM}}^{(p)}$ and $E_{\text{EM}}^{(t)}$ are the poloidal and toroidal magnetic-field energies, respectively, given by

$$E_{\text{EM}}^{(p)} = \frac{16\pi^2 C_1^2}{3} \times \int_0^R \left[e^{-\lambda} \left\{ \frac{d}{dr}(r^2 \psi_1) \right\}^2 + 2e^\lambda r^2 \psi_1^2 \right] dr, \quad (104)$$

$$E_{\text{EM}}^{(t)} = \frac{16\pi^2 C_1^2}{3} \int_0^R L^2 e^{\lambda-2\nu} r^4 \psi_1^2 dr. \quad (105)$$

Multipole moments are also global and physical quantities characterizing the equilibrium star. The constant D appearing in the outer solutions, Equations (96) and (98), is related to the mass quadrupole moment ΔQ , defined by $\Delta Q \equiv 8M^3 D/5$ (see, e.g., Refs. [23, 62]).

Characteristic quantities for the stellar deformation due to magnetic stress also feature the magnetized stars. The surface of the star is defined by $P(r) + (4\pi C_1)^2 (\delta P_0(r) + \delta P_2(r) P_2(\theta)) = 0$. Thus, the radial displacement of the fluid elements on the stellar surface, Δr , is given by

$$\begin{aligned} \Delta r &= (\Delta r)_0 + (\Delta r)_2 P_2(\theta), \\ &= -(4\pi C_1)^2 (\delta P_0(R) + \delta P_2(R) P_2(\theta)) \frac{dr}{dP}(R). \end{aligned} \quad (106)$$

Here, $(\Delta r)_0$ may be interpreted as an average change in the radius of the star induced by the magnetic effects. The degree of the quadrupole surface deformation due to the magnetic stress is well described by the ellipticity, given by

$$e^* = -\frac{3}{2} (4\pi C_1)^2 \left[\frac{(\Delta r)_2}{R} + K_2(R) \right], \quad (107)$$

where e^* is defined as a relative difference between the equatorial and polar circumference radii of the star [23]. Thus, $e^* < 0$ ($e^* > 0$) means that the star is prolate (oblate).

Another physically important quantity of magnetized objects is the total magnetic helicity \mathcal{H} , which is conserved in ideal magnetohydrodynamics, and is defined by

$$\mathcal{H} \equiv \int H^0 \sqrt{-g} d^3x, \quad (108)$$

where H^0 is the time component of the magnetic helicity four-current H^μ , defined by

$$H^\mu \equiv -\frac{1}{2} \epsilon^{\mu\nu\alpha\beta} A_\nu F_{\alpha\beta}. \quad (109)$$

Taking the covariant derivative of Equation (109) yields

$$\nabla_\mu H^\mu = -\frac{1}{2} F^{*\mu\nu} F_{\mu\nu}. \quad (110)$$

Thus, $\nabla_\mu H^\mu = 0$ if $F_{\mu\nu} u^\nu = 0$, i.e., $F^{*\mu\nu} = B^\mu u^\nu - B^\nu u^\mu$, and we confirm that the magnetic helicity \mathcal{H} is a conserved quantity in ideal magnetohydrodynamics. For the present models, the total magnetic helicity is explicitly written as

$$\mathcal{H} = \frac{16\pi}{3} (4\pi C_1)^2 L \int_0^R e^{\lambda-\nu} r^4 \psi_1^2 dr, \quad (111)$$

where the surface boundary condition (63) has been used. The dimensionless magnetic helicity, defined by $\mathcal{H}_M \equiv \mathcal{H}/M^2$, is used when its numerical value is shown. The magnetic helicity is a measure of the net twist of a magnetic-field configuration. Thus, the magnetic helicity vanishes for purely poloidal fields and for purely toroidal fields. Some experiments and numerical computations show an interesting fact that the total magnetic helicity is likely to be conserved even when the resistivity cannot be ignored [40, 63]. If this fact is retained for the neutron star formation process, the total magnetic helicity has to be approximately conserved during its formation process.

V. NUMERICAL RESULTS

In this section, we present some numerical examples of stably stratified stars composed of mixed poloidal-toroidal magnetic fields. As one-parameter equations of state, we employ the following one,

$$P = \kappa \rho^{1 + \frac{1}{n}}, \quad (112)$$

$$\varepsilon = \frac{1}{\Gamma - 1} \frac{P}{\rho}, \quad (113)$$

where κ and n are the polytropic constant and index, respectively, and Γ denotes the adiabatic index, which is defined by $\Gamma = (\partial \ln P / \partial \ln \rho)_S$. κ , n , and Γ are constants and may be specified independently for the construction of equilibrium stars, i.e. Γ is not $1 + 1/n$ in general. We define a general relativistic Schwarzschild discriminant A for non-magnetized spherical stars by

$$A \equiv \frac{1}{\rho h} \frac{d\rho^*}{dr} - \frac{1}{\Gamma} \frac{1}{P} \frac{dP}{dr}, \quad (114)$$

where ρ^* is the total energy density, defined by $\rho^* \equiv \rho + \rho\varepsilon$. Note that there is no unique definition for the general relativistic Schwarzschild discriminant. However, in the present context, only its sign matters. For different definitions of it, see, e.g., Refs. [64–66]. Following Ipson and Lindblom [66], we employ a definition of the Brunt–Väisälä frequency $N \equiv \sqrt{-gA}$ with

$$g \equiv -e^{2(\nu-\lambda)} \frac{1}{\rho h} \frac{dP}{dr}. \quad (115)$$

If there is a region of $A > 0$, the star has an unstably stratified region and becomes convectively unstable

there. For the standard stars whose density profile everywhere satisfies $d\rho/dr < 0$, the condition of the stable stratification for the equations of state (112) and (113) is given by

$$\Gamma > \frac{n+1}{n}. \quad (116)$$

Note that for the isentropic case, defined by $\Gamma = (n+1)/n$, the star is not stratified (marginally stable against convection), as already mentioned.

Hereafter, we consider the $n = 1$ case for simplicity, while we employ $\Gamma = 2$ and 2.1: The $\Gamma = 2$ models are non-stratified ones, whose results are compared with those given in Ref. [23] to check our numerical results. The choice of $\Gamma = 2.1$ comes from the following reason: As argued by Reisenegger and Goldreich [51], the Brunt–Väisälä frequency N from the proton-neutron composition gradient inside neutron stars is approximated by

$$N \approx \sqrt{\frac{x}{2}} \sqrt{\frac{d\rho}{dP}} g, \quad (117)$$

where x denotes the ratio of the number densities of protons to neutrons. From Equation (117), it is found that the $\Gamma = 2.1$ models have Brunt–Väisälä frequencies at the stellar center similar to those of Reisenegger and Goldreich’s models with $x \approx 0.1$, which is a reasonable value for sufficiently cold neutron stars. Note that the origins of the buoyancy in our models and normal neutron stars are different. In our models, the buoyancy results from the entropy gradient not the composition gradient.

First, we describe properties of the unperturbed stars. In the Newtonian framework, the profiles of a star like a density distribution are independent of values of Γ because Newtonian gravity is determined only by the rest mass density and the pressure is assumed to be a function of the rest mass density only. Thus, we may calculate thermodynamical structures of the star like internal energy for any value of Γ after determining the structure of a star. In general relativity, by contrast, the profiles of the star do depend on the value of Γ because P and ε are a source of gravity. Thus, we have to recalculate stellar profiles in general relativity whenever a value of Γ is changed.

In Figure 1, the gravitational mass M and the baryon mass M^* are plotted as functions of the central density of the star $q_0 \equiv \rho(r=0)$. Throughout this paper, we use units of $\kappa = 1$ when showing numerical results. This figure shows that values of M and M^* for the $\Gamma = 2.1$ models are larger than those for the $\Gamma = 2$ models for the same central density. Figure 2 plots relative differences between the $\Gamma = 2.1$ and the $\Gamma = 2$ models in the gravitational mass M , the baryon mass M^* , and the stellar radius R , as functions of the central density q_0 . This shows that the radius of the star increases with increasing Γ if one keeps the central density constant. The reason is that an increase in Γ reduces the total internal energy of the star and leads to a decrease in an effective

TABLE I: Global and physical quantities for the background stars in units of $\kappa = 1$.

Γ	M/R	q_0	M	M^*	$E_{\text{int}}/ W $
2.000	0.1000	0.07027	0.1062	0.1118	0.4078
	0.2000	0.25582	0.1623	0.1780	0.5633
2.100	0.1000	0.06983	0.1066	0.1124	0.3706
	0.2000	0.24893	0.1643	0.1820	0.5104

TABLE II: Dimensionless low-order eigenvalues L_i in units of R^{-1} .

Γ	Mode order	$M/R = 0.1000$	$M/R = 0.2000$
2.000	RL_1	5.792	3.907
	RL_2	8.315	5.601
	RL_3	10.80	7.257
	RL_4	13.26	8.903
	RL_5	15.71	10.54
	RL_6	18.16	12.18
2.100	RL_1	5.787	3.909
	RL_2	8.316	5.619
	RL_3	10.80	7.283
	RL_4	13.26	8.937
	RL_5	15.71	10.59
	RL_6	18.16	12.23

gravitational attraction force. Figure 2 also shows that $\delta M^* > \delta M > \delta R$ for all the values of q_0 calculated in the present study and that a typical value of the relative difference in the baryon mass for a standard neutron star model with $q_0 \approx 0.2$ is within several percents. Thus, we may conclude that the $\Gamma = 2.1$ model has properties quite similar to those of the $\Gamma = 2$ model, except for the stability against convection: We emphasize again that the stratification condition of the $\Gamma = 2.1$ model is absolutely different from that of the $\Gamma = 2$ model. Figures 1 and 2 show that the gravitational mass, baryon mass, and radius of the stars tend to be independent of Γ as $q_0 \rightarrow 0$, i.e., in the Newtonian limit. Henceforth, we will focus on the compact models with $M/R = 0.1$ and 0.2. The models having $M/R = 0.2$ will be a reasonable model of a neutron star. In Table I, some global and physical quantities for the $\Gamma = 2$ and 2.1 models are tabulated.

Next we explore the magnetic-field profile around the background spherical stars and its effects on the stellar structures. As already mentioned in the previous section, the magnetic-field profile is determined by solving an eigenvalue equation with respect to the eigenvalue L , which is related to the toroidal magnetic-field strength through $L = F_{12} \sin \theta e^{\nu-\lambda} \Psi^{-1}$. Then, a discrete sequence of L is allowed for the magnetized stars satisfying the boundary conditions (57) and (63). Table II lists a sequence of the dimensionless eigenvalues L in units of R^{-1} for the first six eigensolutions, where L_i means the i -th eigenvalue L satisfying $0 < L_1 < L_2 < L_3 < \dots$. For the models with $\Gamma = 2$, the values of L in units of R^{-1} are compared with those given in Table I of Ref. [23] and we confirm that our results are in excellent agreement

with theirs.

Here, we should remark the following point. In the study of Ref. [23], the meridional flow is in general present. However, the meridional flow may be absent in the solutions of Ref. [23]. This no meridional-flow limit is given by the limit $|\tilde{C}| \rightarrow \infty$ with \tilde{L} kept to be constant, in the notation of Ref. [23]. Even if we take this limit, the magnetic field remains unchanged (see Equations (83) – (86) of Ref. [23]) although the meridional flow vanishes (see Equations (88) and (89) of Ref. [23]). By using a relation $h e^\nu = \text{const.}$, which is satisfied for non-magnetized “isentropic” spherical stars, we also show for isentropic stars with no meridional flow that basic equations of Ref. [23], (75), (94), (95), and (100) – (103), become equivalent to our basic equations, (56), and (74) – (79) (but note some differences in notation and definition of physical quantities, e.g., their \tilde{L} corresponds to our L). Here, it should be emphasized that the parameter \tilde{C} associated with the strength of the meridional flow does not appear in the equations of Ref. [23], (75), (94), (95), and (100) – (103), which fully determine the structure of magnetized stars with no meridional flow.

Table II shows that the dimensionless eigenvalues $R \times L$ for the $\Gamma = 2.1$ model are approximately equal to those for the $\Gamma = 2$ model. The same result is found in the flux function Ψ if one regards $\Psi(r, \theta)$ as a function of r/R not as r . These facts imply that slight changes in Γ do not affect values of $R \times L$ and $\Psi(r/R, \theta)$ distributions.

Figures 3 and 4 display the profiles of magnetic fields; eigensolutions of Ψ and F_{12} with $L = L_1 - L_6$ for the spherical star with $M/R = 0.2$ and $\Gamma = 2.1$ (see the corresponding eigenvalues in Table II). Figure 3 shows how lines of the magnetic force on the meridional cross section behave, because an equi- Ψ line corresponds to a line of the magnetic force. These figures suggest that higher-order eigensolutions have more non-uniform structures of the magnetic fields. Figure 3 also shows that there is a negative region of Ψ for the models with L_2 , L_4 , and L_6 , while Ψ is everywhere non-negative for the models with $L = L_1$, L_3 , and L_5 .

For analyzing properties of magnetic-field profiles, it is helpful to introduce an orthonormal tetrad component of the magnetic field, B_μ , given by

$$\begin{aligned} B_{(t)} &= 0, \quad B_{(r)} = -8\pi C_1 \psi_1 \cos \theta, \\ B_{(\theta)} &= 4\pi C_1 e^{-\lambda} (r\psi'_1 + 2\psi_1) \sin \theta, \\ B_{(\phi)} &= 4\pi C_1 e^{-\nu} L r \psi_1 \sin \theta. \end{aligned} \quad (118)$$

Then, we can define that $B_c \equiv |B(r=0)| = 8\pi C_1 \psi_1(0)$. As mentioned before, profiles of $B_{(\mu)}$ for the $\Gamma = 2.1$ models are very similar to those for the $\Gamma = 2$ models. Their difference cannot be visible if $B_{(\mu)}$ are plotted as functions of r/R in the same figure even though no figure is given in this paper. To show the dimensionless total magnetic helicity of the magnetized stars, \mathcal{H}_M , we follow Ioka and Sasaki [23] and use a dimensionless parameter

that represents magnetic-field strength, defined by

$$\mathcal{R}_M \equiv \frac{B_c^2 R^4}{4M^2}, \quad (119)$$

which is as large as the ratio of the magnetic energy to the gravitational energy.

Table III lists global physical quantities characterizing the magnetized stars with mixed poloidal-toroidal fields; the changes in the central density $\Delta\rho_c$, the gravitational mass ΔM , the quadrupole moment ΔQ , the mean radius $(\Delta r)_0$, the ellipticity e^* , the magnetic helicity \mathcal{H}_M , the magnetic energy E_{EM} , and the ratio of the poloidal magnetic energy $E_{\text{EM}}^{(p)}$ to the total magnetic energy E_{EM} . In this table, the results for the first six eigensolutions are shown and all the quantities are normalized to be non-dimensional, as given in the first row. By comparing the results shown in Table III with those in Table 2 of Ref. [23], we can again check the reliability of our results; ours are in agreement with theirs for the $\Gamma = 2$ models in an acceptable level.

Although there are slight numerical differences between them, there is no qualitative difference between the results of the $\Gamma = 2.1$ and $\Gamma = 2$ models (see Table III). Thus, basic properties of the magnetized star described in Ref. [23] hold for the present $\Gamma = 2.1$ models, although the convective stability is different and also any meridional flow is absent in the present models. For the magnetized-star sequences, characterized by the fixed baryon mass and magnetic helicity, shown in Table III, the total gravitational mass and the total magnetic energy increase with the mode number i (or the eigenvalue L). This property is reasonable due to the following reason: As found in Figures 3 and 4, higher-order eigensolutions, characterized by a larger eigenvalue, have more non-uniform structures of the magnetic fields, which can usually store larger magnetic-field energy. From Table III, we also find that all the models obtained in this study are toroidal-magnetic-field dominant and that the value of $E_{\text{EM}}^{(p)}/E_{\text{EM}}$ decreases as the mode number i increases. The latter property is well explained by the fact that L is interpreted as the ratio of the toroidal magnetic-field strength to the poloidal magnetic-field one, and it increases as the mode number i increases. The magnetic hoop stress around the symmetry axis due to the toroidal magnetic field tends to make the star prolate like a rubber belt fastening a waist of the star. This is consistent with the facts that all the stars obtained in this study have negative ellipticity e^* , i.e., the star is prolate, and that the degree of the quadrupole deformation measured by $|e^*|$ becomes more pronounced for higher-order solutions, as shown in Table III.

VI. DISCUSSION: THE STABILITY OF THE STARS

Checking the stability is an important issue to be explored after obtaining an equilibrium state of a magne-

TABLE III: Global and physical quantities characterizing the magnetized stars with mixed poloidal-toroidal fields; the changes in the central density $\Delta\rho_c$, the gravitational mass ΔM , the quadrupole moment ΔQ , the mean radius $(\Delta r)_0$, the ellipticity e^* , the magnetic helicity \mathcal{H}_M , the magnetic energy E_{EM} , and the ratio of the poloidal magnetic energy $E_{EM}^{(p)}$ to the total magnetic energy E_{EM} . Here, all the quantities are normalized to be non-dimensional, as given in the first row.

$(\Gamma, M/R)$	L	$\Delta\rho_c/q_0\mathcal{H}_M$	$\Delta M/M\mathcal{H}_M$	$\Delta Q/MR^2\mathcal{H}_M$	$(\Delta r)_0/R\mathcal{H}_M$	e^*/\mathcal{H}_M	$\mathcal{H}_M/\mathcal{R}_M$	$E_{EM}/ W \mathcal{H}_M$	$E_{EM}^{(p)}/E_{EM}$
(2, 0.2)	L_1	0.2545	2.446×10^{-2}	-6.163×10^{-3}	-2.601×10^{-2}	-1.505×10^{-2}	2.556×10^{-1}	0.1903	0.3684
	L_2	0.4063	3.067×10^{-2}	-1.875×10^{-2}	9.007×10^{-2}	-4.580×10^{-2}	4.346×10^{-1}	0.2222	0.2785
	L_3	0.5307	3.634×10^{-2}	-3.293×10^{-2}	4.156×10^{-2}	-8.043×10^{-2}	1.153×10^{-1}	0.2606	0.2097
	L_4	0.6736	4.202×10^{-2}	-4.719×10^{-2}	7.387×10^{-2}	-1.153×10^{-2}	1.690×10^{-1}	0.3000	0.1607
	L_5	0.7967	4.780×10^{-2}	-6.120×10^{-2}	1.051×10^{-1}	-1.495×10^{-1}	7.632×10^{-2}	0.3404	0.1255
	L_6	0.9303	5.372×10^{-2}	-7.490×10^{-2}	1.353×10^{-1}	-1.829×10^{-1}	1.026×10^{-1}	0.3818	0.09996
(2, 0.1)	L_1	-0.04212	1.777×10^{-2}	-1.957×10^{-2}	9.053×10^{-2}	-3.654×10^{-2}	2.777×10^{-1}	0.2488	0.3541
	L_2	0.1186	2.223×10^{-2}	-6.018×10^{-2}	1.845×10^{-1}	-1.123×10^{-1}	5.802×10^{-1}	0.3043	0.2588
	L_3	0.1856	2.650×10^{-2}	-1.036×10^{-1}	2.797×10^{-1}	-1.935×10^{-1}	1.349×10^{-1}	0.3612	0.1913
	L_4	0.3061	3.074×10^{-2}	-1.467×10^{-1}	3.733×10^{-1}	-2.738×10^{-1}	2.208×10^{-1}	0.4188	0.1444
	L_5	0.3825	3.507×10^{-2}	-1.886×10^{-1}	4.649×10^{-1}	-3.521×10^{-1}	9.250×10^{-2}	0.4777	0.1116
	L_6	0.4846	3.953×10^{-2}	-2.295×10^{-1}	5.547×10^{-1}	-4.284×10^{-1}	1.338×10^{-1}	0.5378	0.08816
(2.1, 0.2)	L_1	0.2227	2.417×10^{-2}	-6.186×10^{-3}	-1.747×10^{-2}	-1.511×10^{-2}	2.571×10^{-1}	0.1912	0.3694
	L_2	0.3599	3.047×10^{-2}	-1.892×10^{-2}	2.124×10^{-2}	-4.622×10^{-2}	4.146×10^{-1}	0.2245	0.2810
	L_3	0.4711	3.604×10^{-2}	-3.340×10^{-2}	5.790×10^{-2}	-8.158×10^{-2}	1.146×10^{-1}	0.2632	0.2120
	L_4	0.6008	4.162×10^{-2}	-4.800×10^{-2}	9.407×10^{-2}	-1.172×10^{-1}	1.638×10^{-1}	0.3029	0.1627
	L_5	0.7115	4.730×10^{-2}	-6.233×10^{-2}	1.292×10^{-1}	-1.523×10^{-1}	7.549×10^{-2}	0.3435	0.1272
	L_6	0.8324	5.311×10^{-2}	-7.635×10^{-2}	1.631×10^{-1}	-1.865×10^{-1}	9.981×10^{-2}	0.3851	0.1014
(2.1, 0.1)	L_1	-0.03900	1.852×10^{-2}	-1.952×10^{-2}	8.932×10^{-2}	-3.643×10^{-2}	2.777×10^{-1}	0.2490	0.3545
	L_2	0.1208	2.319×10^{-2}	-6.015×10^{-2}	1.832×10^{-1}	-1.122×10^{-1}	5.680×10^{-1}	0.3050	0.2597
	L_3	0.1884	2.763×10^{-2}	-1.038×10^{-1}	2.783×10^{-1}	-1.938×10^{-1}	1.343×10^{-1}	0.3620	0.1921
	L_4	0.3091	3.205×10^{-2}	-1.470×10^{-1}	3.719×10^{-1}	-2.745×10^{-1}	2.177×10^{-1}	0.4196	0.1451
	L_5	0.3861	3.655×10^{-2}	-1.892×10^{-1}	4.634×10^{-1}	-3.531×10^{-1}	9.192×10^{-2}	0.4786	0.1122
	L_6	0.4885	4.120×10^{-2}	-2.302×10^{-1}	5.531×10^{-1}	-4.298×10^{-1}	1.321×10^{-1}	0.5388	0.08865

tized star, because unstable solutions lose their physical meaning in the sense that they are not realized in nature. For the present models, as observed in Sec. V, the gravitational mass and the total electromagnetic energy increase with the mode number i of the eigensolution, if we consider the equilibrium sequences for a given baryon mass and a magnetic helicity. This result is quite important and interesting due to the following reason. If the total baryon mass and magnetic helicity are conserved during the formation process of neutron stars, as discussed before, it is likely that the final state of the magnetic fields characterized by the arbitrary functions of the flux function (46) – (48) and the surface boundary condition (63) is the lowest-order eigensolution characterized by the smallest eigenvalue $L = L_1$ because it has the lowest gravitational mass and total electromagnetic energy among the equilibrium solutions characterized by the fixed baryon mass and magnetic helicity. We therefore conjecture that all the high-order solutions are unstable because there is an equilibrium state with energy lower than theirs and that the solutions associated with the lowest eigenvalue $L = L_1$ can be stable if there is a stable solution among the present models. Another important fact is that for the magnetic-field profile characterized by $L = L_1$, their magnetic energy is most equally divided into the poloidal and the toroidal magnetic en-

ergies among the eigensolutions. This property is consistent with the conjecture for stable magnetic configurations given by the linear analyses; stable magnetized stars contain both poloidal and toroidal components with comparable magnetic energies.

Most of the magnetized-star models constructed in the framework of general relativity so far were non-stratified, and therefore, marginally stable against convection. Those non-stratified models are in general highly unstable against the magnetic buoyancy in the vicinity of the stellar surface, in the presence of magnetic fields. For strongly magnetized stars like magnetars, as shown by Kiuchi et al. [48], the magnetic buoyancy instability induces a convective motion near the surface of the star and fully destroys initially coherent magnetic fields inside the star. To stabilize this magnetic-buoyancy instability, the stratification with the strength sufficient to overcome the magnetic buoyancy are necessary as a stabilizing agent. This stabilization effect prevails in non-rotating diffusionless stars with purely toroidal magnetic fields as argued by Acheson [35]. When $N^2 \gg \omega_A^2 > 0$, his dispersion relation (see Equation (3.20) of Ref. [35]) has four solutions, $\omega \approx \pm k_\theta N(k_r^2 + k_\theta^2)^{-\frac{1}{2}}$ and $\omega \approx \pm m\omega_A$, where ω and ω_A mean the oscillation and the Alfvén frequencies, respectively, and k_r , k_θ , and m denote the vertical, horizontal, and azimuthal wave numbers, respec-

tively. These four solutions are composed of propagating waves; the former is an internal gravity wave and the latter an Alfvén wave. We therefore confirm that there is no magnetic-buoyancy instability as long as $N^2 \gg \omega_A^2 > 0$. In Figure 5, we plot squares of the Brunt–Väisälä frequency N^2 and the Alfvén frequency ω_A^2 for a $\Gamma = 2.1$ model characterized by $M/R = 0.2$ and $L = L_1$ as functions of the dimensionless radius r/R . Here, the Alfvén frequency is evaluated on the equatorial plane and defined by $\omega_A \equiv \sqrt{B^\mu B_\mu / ((4\pi\rho h + B^\mu B_\mu)r^2)}$, and the strength of the magnetic fields is determined by the condition $E_{\text{EM}}/|W| = 2.5 \times 10^{-2}$, which corresponds to very strong magnetic fields $\approx 10^{16}$ G for a typical neutron star. This figure shows that the Brunt–Väisälä frequency, N , is much larger than the Alfvén frequency ω_A in the region of $r > 0.5R$ for the models with $L = L_1$. Thus, we can predict that this model is stable against the magnetic buoyancy vicinity of the stellar surface. It should be noted that the physical origin of the anti-buoyancy force in our models is different from that in real neutron stars, as mentioned before, because the former comes from the entropy gradient and the later mainly from the composition gradient (see, e.g., Ref. [51]). Magnetic fields, however, do not care the origin of the anti-buoyancy force, but do whether stars are stably stratified or not.

As pointed out by Acheson [36], the magnetic hoop stress caused by the strong toroidal magnetic fields governs dynamics of the perturbation near the center of the star. This fact may be confirmed from Figure 5, which shows $N \ll \omega_A$ near the center of the star. Thus, the stratification is not helpful near the center of the star in the presence of the magnetic instability. For the central part of the star, as mentioned before, the presence of the poloidal magnetic fields having comparable strength with the toroidal ones will suppress the pinch-type instabilities. By solving linear perturbation equations around magnetized star models in the framework of Newtonian dynamics, Lander and Jones showed that this suppression of the magnetic instability indeed occurs, although the presence of the poloidal magnetic fields leads another instability associated with themselves [46] (see, also, Refs. [38, 39]). Thus, the results of their numerical simulation lessen the possibility that the pinch-type magnetic instabilities are completely removed for the stars containing the mixed poloidal-toroidal magnetic fields with comparable strength. Although Lander and Jones’s results obviously conflict with those by Braithwaite and his collaborators [40–43], we have so far had no definite conclusion to this controversy. One important difference between their analyses is in the treatment of the resistivity of the matter; Lander and Jones employed the ideal magnetohydrodynamics approximation, whereas Braithwaite and his collaborators took into account the resistivity. This might be a key to the solution of this problem. Toward a definite answer to this stability problem, we need further studies on the stability of the magnetized stars.

As such a study, we plan to perform a stability anal-

ysis of the present magnetized star models by general relativistic magnetohydrodynamics simulations like those done by Kiuchi et al. [47, 48]. The present stably stratified models characterized by $L = L_1$ satisfy the following conditions; they have both poloidal and toroidal magnetic fields with comparable strength to suppress the hoop-stress instability inside the star, and in addition, the fluid constructing the magnetized star is stably stratified with strength sufficient to overcome the magnetic buoyancy near the stellar surface. Thus, it is obvious that some major magnetic instabilities will be reduced in the present magnetized star models. This will make the stability problem more tractable.

As discussed in Kiuchi et al. [22, 47], it is reasonable to expect that the toroidal component of the magnetic fields is much larger than the poloidal component inside the neutron star at least soon after its birth. The reason for this is that the winding of poloidal magnetic fields caused by a rapid and differential rotation during the core collapse would create large toroidal fields. Most of general relativistic magnetized star models obtained in numerical computations so far can, however, have toroidal magnetic fields much weaker than poloidal ones [24–26]. Their minimum ratio of the poloidal magnetic field energy to the total magnetic energy is ≈ 0.92 , which is much larger than those of the present models. (For magnetized star models in the framework of the Newtonian dynamics, see, e.g., Ref. [67]). Their magnetic fields are composed of the mixed poloidal–toroidal twisted torus magnetic fields inside the star and nearly dipolar magnetic fields outside the star. They may look quite plausible for the magnetosphere of neutron stars. However, weak toroidal magnetic-field strength seems to be unlikely for the strongly magnetized neutron stars. Although the magnetic field vanishes outside the star for the present models, which is quite unrealistic, the present models would give a reasonable inside structure of the strongly magnetized neutron stars because of their large toroidal magnetic-field strength. For obtaining more realistic models composed of a stably stratified fluid, basic equations given in Equations (19) – (25) may be employed as far as ideal magnetohydrodynamics and the barotropic equations of state are employed.

VII. SUMMARY

We constructed the magnetized stars composed of a stratified fluid in the framework of general relativity. By assuming ideal magnetohydrodynamics and employing a barotropic equation of state, we first derive basic equations for describing stably stratified stationary axisymmetric stars containing both poloidal and toroidal magnetic fields. As sample models, the magnetized star considered by Ioka and Sasaki [23] are modified to the ones stably stratified. The resulting models have both poloidal and toroidal magnetic fields with comparable strength. The magnetized stars newly constructed in this study

are believed to be more stable than the existing relativistic models because they have both poloidal and toroidal magnetic fields with comparable strength, and the magnetic buoyancy instability near the surface of the star, which can be stabilized by the stratification, are suppressed.

Acknowledgments

S.Y. thanks U. Lee for fruitful discussions. This work was supported by Grant-in-Aid for Scientific Research

(22740178, 21340051, 24244028, 24540245) and Grant-in-Aid on Innovative Area (20105004), and HPCI Strategic Program in Japan MEXT.

-
- [1] R. C. Duncan and C. Thompson, *Astrophys. J.* **392**, L9 (1992).
 - [2] B. Paczyński, *Acta Astron.* **42**, 145 (1992).
 - [3] C. Thompson and R. C. Duncan, *Mon. Not. R. Astro. Soc.* **275**, 255 (1995).
 - [4] C. Thompson and R. C. Duncan, *Astrophys. J.* **473**, 322 (1996).
 - [5] P. M. Woods and C. Thompson, in *Compact stellar X-ray sources*, edited by W. Lewin and M. van der Klis (Cambridge University Press, Cambridge, 2006).
 - [6] S. Chandrasekhar and E. Fermi, *Astrophys. J.* **118**, 116 (1953).
 - [7] K. H. Prendergast, *Astrophys. J.* **123**, 498 (1956).
 - [8] L. Woltjer, *Astrophys. J.* **131**, 227 (1960).
 - [9] I. W. Roxburgh, *Mon. Not. R. Astro. Soc.* **132**, 347 (1966).
 - [10] J. J. Monaghan, *Mon. Not. R. Astro. Soc.* **131**, 105 (1965).
 - [11] K. Ioka, *Mon. Not. R. Astro. Soc.* **327**, 639 (2001).
 - [12] M. J. Miketinac, *Ap&SS*, **22**, 413 (1973).
 - [13] M. J. Miketinac, *Ap&SS*, **35**, 349 (1975).
 - [14] Y. Tomimura and Y. Eriguchi, *Mon. Not. R. Astro. Soc.* **359**, 1117 (2005).
 - [15] S. Yoshida and Y. Eriguchi, *Astrophys. J. Suppl.* **164**, 156 (2006).
 - [16] S. Yoshida, S. Yoshida and Y. Eriguchi, *Astrophys. J.* **651**, 462 (2006).
 - [17] S. K. Lander and D. I. Jones, *Mon. Not. R. Astro. Soc.* **395**, 2162 (2009).
 - [18] V. Duez and S. Mathis, *Astron. Astrophys.* **517**, A58 (2010).
 - [19] M. Bocquet, S. Bonazzola, E. Gourgoulhon, and J. Novak, *Astron. Astrophys.* **301**, 757 (1995).
 - [20] C. Y. Cardall, M. Prakash, and M. Lattimer, *Astrophys. J.* **554**, 322 (2001).
 - [21] K. Konno, T. Obata, and Y. Kojima, *Astron. Astrophys.* **352**, 211 (1999).
 - [22] K. Kiuchi and S. Yoshida, *Phys. Rev. D* **78**, 044045 (2008).
 - [23] K. Ioka and M. Sasaki, *Astrophys. J.* **600**, 296 (2004).
 - [24] A. Colaiuda, V. Ferrari, L. Gualtieri, and J. A. Pons, *Mon. Not. R. Astro. Soc.* **385**, 2080 (2008).
 - [25] R. Ciolfi, V. Ferrari, L. Gualtieri, and J. A. Pons, *Mon. Not. R. Astro. Soc.* **397**, 913 (2009).
 - [26] R. Ciolfi, V. Ferrari, and L. Gualtieri, *Mon. Not. R. Astro. Soc.* **406**, 2540 (2010).
 - [27] R. J. Tayler, *Mon. Not. R. Astro. Soc.* **161**, 365 (1973).
 - [28] G. A. E. Wright, *Mon. Not. R. Astro. Soc.* **162**, 339 (1973).
 - [29] P. Markey and R. J. Tayler, *Mon. Not. R. Astro. Soc.* **163**, 77 (1973).
 - [30] R. J. Tayler, *Mon. Not. R. Astro. Soc.* **191**, 151 (1980).
 - [31] W. V. Asche, R. J. Tayler, and M. Gossens, *Astron. Astrophys.* **109**, 166 (1982).
 - [32] E. Flowers and M. A. Ruderman, *Astrophys. J.* **215**, 302 (1977).
 - [33] E. Pitts and R. J. Tayler, *Mon. Not. R. Astro. Soc.* **216**, 139 (1986).
 - [34] M. Goossens, D. Biront, and R. J. Tayler, *Astrophys. Space Sci.* **75**, 521 (1981).
 - [35] D. J. Acheson, *Phil. Trans. Roy. Soc. London A* **289**, 459 (1978).
 - [36] D. J. Acheson, *Solar Phys.* **62**, 23 (1979).
 - [37] H. C. Spruit, *Astron. Astrophys.* **349**, 189 (1999).
 - [38] A. Bonanno and V. Urpin, *Astron. Astrophys.* **477**, 35 (2008).
 - [39] A. Bonanno and V. Urpin, *Astron. Astrophys.* **488**, 1 (2008).
 - [40] J. Braithwaite and H. C. Spruit, *Nature* **431**, 819 (2004).
 - [41] J. Braithwaite and H. C. Spruit, *Astron. Astrophys.* **450**, 1097 (2006).
 - [42] J. Braithwaite, *Mon. Not. R. Astro. Soc.* **397**, 763 (2009).
 - [43] V. Duez, J. Braithwaite, and S. Mathis, *Astrophys. J.*, **724**, L34 (2010).
 - [44] S. K. Lander and D. I. Jones, *Mon. Not. R. Astro. Soc.* **412**, 1730 (2011).
 - [45] S. K. Lander and D. I. Jones, *Mon. Not. R. Astro. Soc.* **412**, 1394 (2011).
 - [46] S. K. Lander and D. I. Jones, arXiv: 1202.2339 [astro-ph.SR].
 - [47] K. Kiuchi, M. Shibata, and S. Yoshida, *Phys. Rev. D* **78**, 024029 (2008).
 - [48] K. Kiuchi, S. Yoshida, and M. Shibata, *Astron. Astrophys.* **538**, A30 (2011).
 - [49] P. D. Lasky, B. Zink, K. D. Kokkotas, and K. Glampedakis, *Astrophys. J.* **735**, L20 (2011).
 - [50] R. Ciolfi, S. K. Lander, G. M. Manca, and L. Rezzolla, *Astrophys. J.* **736**, L6 (2011).
 - [51] A. Reisenegger and P. Goldreich, *Astrophys. J.* **395**, 240 (1992).
 - [52] L. S. Finn, *Mon. Not. R. Astro. Soc.* **227**, 265 (1987).
 - [53] D. Lai, *Mon. Not. R. Astro. Soc.* **270**, 611 (1994).

- [54] A. Reisenegger, arXiv:0802.2227 (2008).
- [55] E. N. Parker, *Astrophys. J.* **145**, 811 (1966).
- [56] A. Mastrano, A. Melatos, A. Reisenegger, T. Akgün, *Mon. Not. R. Astro. Soc.* **417**, 2288 (2012).
- [57] S. K. Lander, N. Andersson, K. Glampedakis, *Mon. Not. R. Astro. Soc.* **419**, 732 (2012).
- [58] K. Glampedakis, N. Andersson, S. K. Lander, *Mon. Not. R. Astro. Soc.* **420**, 1263 (2012).
- [59] E. Gourgoulhon, C. Markakis, K. Uryu and Y. Eriguchi, *Phys. Rev. D* **83** 104007 (2011).
- [60] R. V. E. Lovelace, C. Mehanian, C. M. Mobarry, and M. E. Sulkanen, *Astrophys. J. Suppl.* **62**, 1 (1986).
- [61] C. W. Misner and K. S. Thorne, and J. A. Wheeler, *Gravitation* Freeman, New York.
- [62] K. P. Thorne, *Rev. Mod. Phys.* **52**, 299 (1980).
- [63] S. Hsu and P. A. Bellan, *Mon. Not. R. Astro. Soc.* **334**, 275 (2002).
- [64] K. S. Throne, *Astrophys. J.* **144**, 201 (1966).
- [65] P. N. McDermott, H. M. Van Horn, and J. F. Scholl, *Astrophys. J.* **268**, 837 (1983).
- [66] J. R. Ipser and L. Lindblom, *Astrophys. J.* **389**, 392 (1992).
- [67] B. Haskell, L. Samuelsson, K. Glampedakis, and N. Andersson, *Mon. Not. R. Astro. Soc.* **385**, 531 (2008).

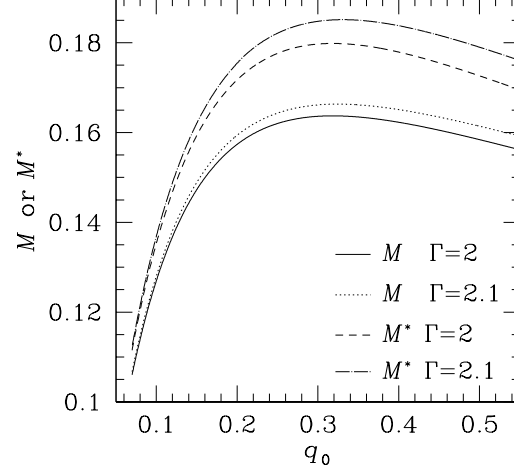


FIG. 1: Gravitational mass M and baryon mass M^* , given as functions of the central density q_0 .

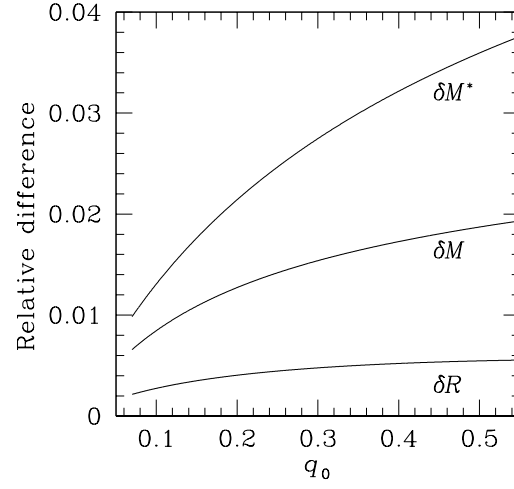


FIG. 2: Relative differences of the gravitational mass M , the baryon mass M^* , and the radius R , given as a function of the central density q_0 . Here, the relative difference of the physical quantity $Q[\Gamma]$ is defined by $\delta Q \equiv 2(Q[2.1] - Q[2]) / (Q[2.1] + Q[2])$.

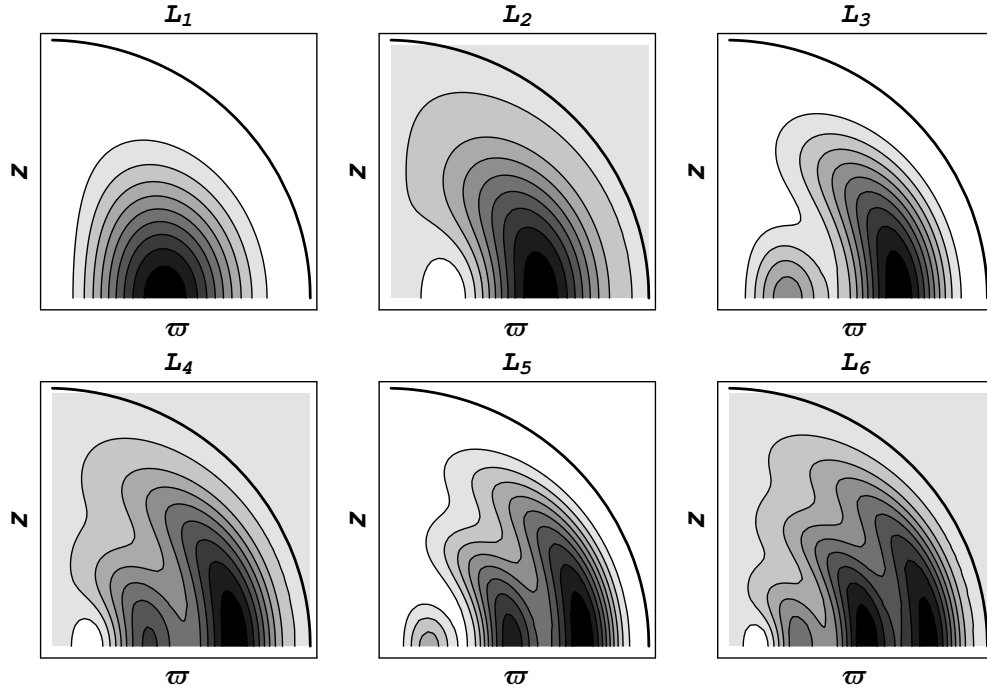


FIG. 3: Equi- Ψ contours on the meridional cross section for the models characterized by $L = L_1, L_2, L_3, L_4, L_5$, and L_6 . Here, z and ϖ are defined by $z \equiv r \cos \theta$ and $\varpi = r \sin \theta$, respectively. The thick quarter circle shows the surface of the star, on which $\Psi = 0$ is, by the boundary condition, required. The black and white regions, respectively, correspond to the maximum and minimum values of Ψ . Since Ψ vanishes outside the star, it can be seen that there is a negative region of Ψ for the models with L_2, L_4 , and L_6 , while Ψ is always positive for the models with $L = L_1, L_3$, and L_5 .

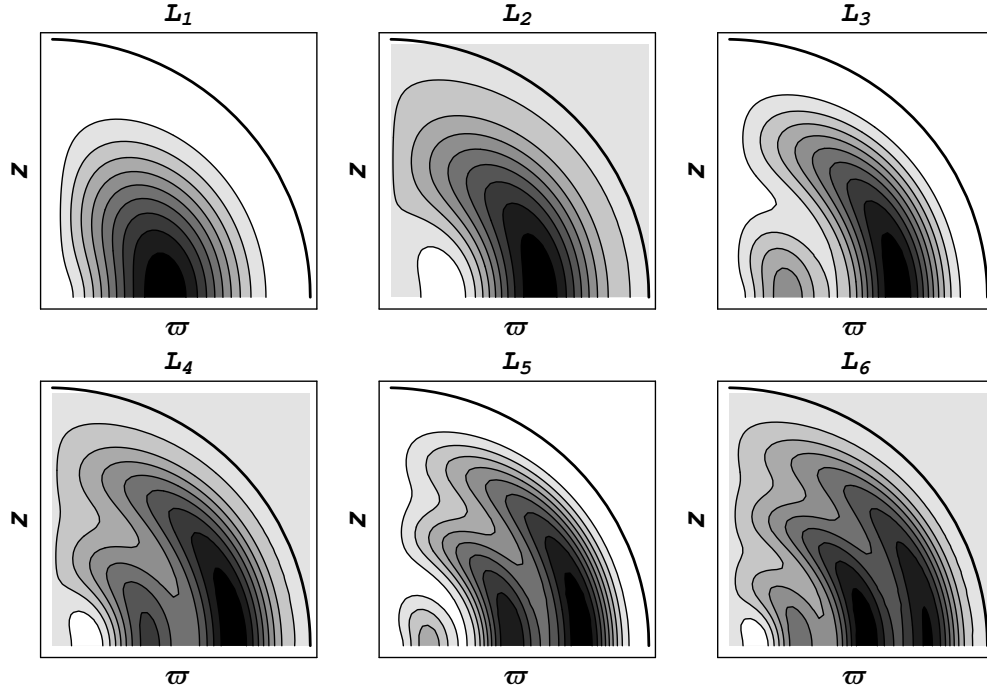


FIG. 4: Equi- F_{12} contours on the meridional cross section for the models characterized by $L = L_1, L_2, L_3, L_4, L_5$, and L_6 . Here, z and ϖ are defined by $z \equiv r \cos \theta$ and $\varpi = r \sin \theta$, respectively. The thick quarter circle shows the surface of the star, on which $F_{12} = 0$ is, by the boundary condition, required. The black and white regions, respectively, correspond to the maximum and minimum values of F_{12} . Since F_{12} vanishes outside the star, it can be seen that there is a negative region of F_{12} for the models with L_2, L_4 , and L_6 , while F_{12} is always positive for the models with $L = L_1, L_3$, and L_5 .

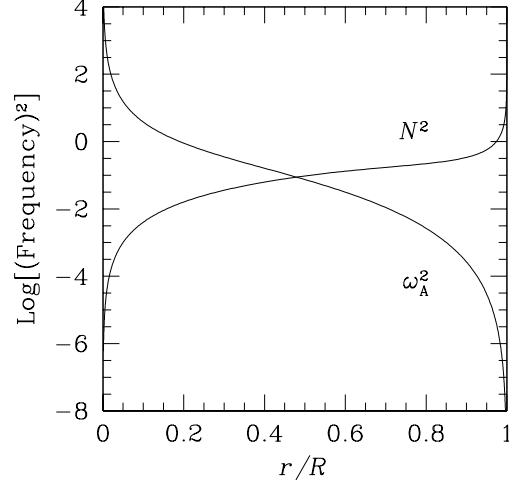


FIG. 5: Squares of the Brunt–Väisälä frequency N^2 and the Alfvén frequency ω_A^2 , given as functions of the dimensionless radius r/R . Here, the Alfvén frequency is defined by $\omega_A \equiv \sqrt{B^\mu B_\mu / ((4\pi\rho h + B^\mu B_\mu)r^2)}$ and evaluated on the equatorial plane ($\theta = \pi/2$), and the strength of the magnetic fields are determined by the condition $E_{\text{EM}}/|W| = 2.5 \times 10^{-2}$.